

OPTIMIZATION METHOD FOR ENERGY CONSUMPTION AND RUNNING TIME OF URBAN RAIL TRAINS BASED ON FNN-PSO-PPO

Nan XIAO*, Guokun XIE, Man JIANG¹

In response to the problems of traditional urban rail train energy consumption optimization methods relying on precise physical parameters, difficult to handle dynamic disturbances, and insufficient adaptability of existing static optimization strategies, a research proposes an integrated optimization model based on feedforward neural network-particle swarm algorithm-proximal strategy optimization. This method constructs a high-precision energy consumption prediction model through a feedforward neural network, combines an improved particle swarm algorithm to achieve static optimization of interval running time, and uses proximal strategy optimization for dynamic strategy adjustment. The experimental results show that under normal operating conditions, the average energy consumption of the model is reduced to 28.5 kWh, a decrease of 20.2% compared to traditional physical models, with a time deviation of only 1.2 seconds. In dynamic disturbance scenarios, the fluctuation amplitude of energy consumption is controlled at +6.2%, and the recovery time is shortened to 3.1 minutes. In actual testing, the one-way energy consumption decreases by 13.6%-16.8%, the on-time rate increases to 99.2%, and the annual comprehensive economic benefit reaches 14.11 million yuan. Overall, this model significantly improves the energy efficiency and operational stability of urban rail trains, and has high engineering application value.

Keywords: Urban rail transit; Energy consumption optimization; Feedforward neural network; Particle swarm optimization; Proximal strategy optimization

1. Introduction

As urban rail transit (URT) networks rapidly expand, the energy efficiency of subway systems, as the backbone of modern urban public transportation, is increasingly receiving attention. Driven by the concept of sustainable development and green transportation construction, optimizing energy consumption (EC) and improving operational efficiency of train operation have become key problems that urgently need to be solved in the field of rail transit. In recent years, many scholars have attempted to introduce intelligent algorithms to achieve multi-objective balancing during train operation. Scholars Hasanzadeh S et al. designed a comprehensive modeling method for optimizing the EC of electric railway systems.

* Corresponding author, e-mail: xiaonan-xn@outlook.com

¹ Public Course Department, Xi'an Traffic Engineering University, Xi'an, 710300, China

This model takes into account various influencing factors, including the slope of different routes, speed restrictions on each section, and the time interval for trains to arrive at each station. Furthermore, the raised scheduling scheme was implemented on Line 2 of the Tehran Urban and Suburban Railway Operation Company, and the findings demonstrated that the scheme had the potential to reduce EC by 3.2% in comparison with the existing train timetable [1]. Scholar Cao Y et al. designed a trajectory optimization method for high-speed trains, aimed at reducing traction EC and improving ride comfort. In addition, this method also achieved energy saving by optimizing the running time between stations [2]. Scholars Novak H et al. proposed an energy-saving train operation control system that includes a detailed train motion model and energy efficiency of the train traction system. By obtaining the parameters of an industrial manufacturer's electric train, a segmented affine train model was constructed to solve the problem of high EC during train operation and improve passenger comfort [3]. Scholar Su S et al. developed an optimized train driving strategy grounded on the Soft Actor-Critic (SAC) method to deal with the control problem of energy-saving trains. The findings indicated that the SAC-based approach exhibited the potential to curtail EC by approximately 1.65%. The application of the proposed method to multiple intervals resulted in a 6.49% reduction in EC [4].

Whilst earlier studies have yielded certain outcomes, there remains scope for enhancement. Most current optimization methods are limited to specific routes or fixed operating conditions, and their generalization ability is difficult to cope with the challenges brought by diverse operating environments. More importantly, EC optimization and runtime control are often treated separately in existing models, lacking effective collaborative mechanisms to achieve dynamic balance between the two. When facing sudden disturbances such as sudden changes in passenger flow and equipment failures, traditional optimization strategies are difficult to handle in a timely manner and cannot provide real-time performance guarantees for the system. In addition, there are obvious shortcomings in the computational efficiency and engineering feasibility of existing intelligent algorithms, which to some extent limit their potential applications in practical operations. Based on this, a research proposed an optimization model that integrates Feedforward Neural Network (FNN), Particle Swarm Optimization (PSO), and Proximal Policy Optimization (PPO) to accelerate the growth of green and low-carbon transportation systems. The innovation of this method lies in: (1) Proposing an FNN-PSO-PPO three-level collaborative optimization architecture to achieve full process optimization from EC prediction to dynamic control. (2) Design a dual constraint handling mechanism with adaptive capability to solve the constraint satisfaction problem in discrete time adjustment. Overall, the research provides new optimization ideas for the intelligent operation of URT.

2. Methods and materials

2.1. Construction of Energy Consumption Model for Urban Rail Trains Based on FNN

The accurate calculation of train traction EC is a critical foundation for energy-saving optimization of URT. The traditional EC modeling methods are mainly divided into two categories: one is the dynamic modeling method grounded on physical laws, and the other is the regression analysis method grounded on statistics. The dynamic modeling method mainly calculates EC by establishing a train force balance equation. Although the physical meaning is clear, its calculation accuracy heavily depends on the accuracy of train parameters, and it is also difficult to handle nonlinear relationships under complex working conditions. Although statistical regression methods reduce dependence on physical parameters, they cannot capture the complex mapping relationships between high-dimensional features. As a deep learning model, FNN exhibits both robust nonlinear fitting capabilities and the advantage of automatic feature extraction. The specific structure can be seen in Fig. 1.

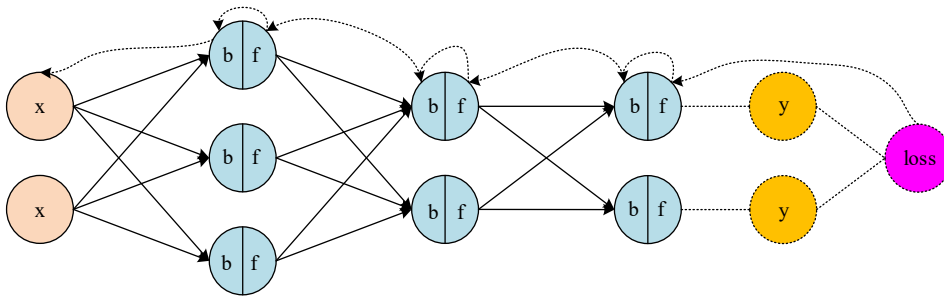


Fig. 1 FNN structure (Fig. source: self drawn by the author)

Fig. 1 shows the specific architecture of FNN. From the Fig., FNN mainly contains an input layer, a hidden layer, and an output layer, which together form a multi-layer perceptron structure. This structure can achieve layer by layer abstraction of high-dimensional input features through hidden layers, and optimize network parameters using backpropagation [5-6]. It is precisely because of this structure that FNN can automatically learn nonlinear features under complex working conditions without the need for precise physical parameters to build mapping relationships between inputs and outputs. Meanwhile, it can also improve expression ability by increasing network depth. Based on this, the study proposed using FNN to construct an EC model for URT. In the design of input features, the model mainly considers information from two dimensions. One dimension is the speed characteristics of train operation, specifically selecting the current time t and the speed observation values before and after 2 seconds (a total of 41 time points, with a sampling interval of 0.1s) to form a 41-dimensional speed sequence. The

other is the line feature, which includes two parameters: equivalent slope and equivalent curvature radius. Therefore, the input feature vector of the input layer can be expressed as formula (1).

$$\mathbf{X} = [v(t - 20\Delta t), \dots, v(t), \dots, v(t + 20\Delta t), i_{eq}, R_{eq}]^T \in \mathbb{R}^{43} \quad (1)$$

In formula (1), \mathbf{X} represents the input feature vector, $v(t)$ represents the train running speed at time t , Δt means the sampling time interval, i_{eq} represents the equivalent slope, and R_{eq} represents the equivalent curvature radius. Considering that there may be some noise in the measurement; to eliminate the measurement noise, the sliding average filtering preprocessing of the input velocity sequence is studied. The specific process is denoted in Fig. 2.

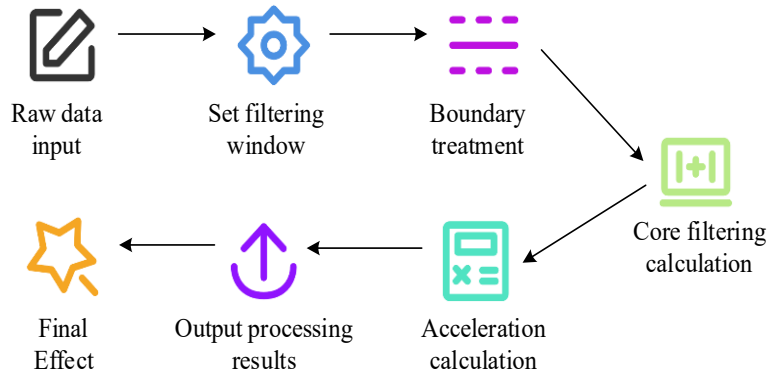


Fig. 2 Preprocessing process of sliding average filtering for velocity sequence (Fig. source: <https://freeicons.io/iconset/free-icons-set>)

Fig. 2 shows the preprocessing process of velocity sequence sliding average filtering. From the Fig., the process first obtains the original running speed data of the train, which is collected at fixed time intervals [7]. Then, it sets a symmetrical sliding window containing two sampling points before and after the current time, with each sampling point assigned the same weight. Next, the starting point of the data sequence is processed. The initial point is taken as the mean of the first two sampling points, the subsequent point is taken as the mean of the first three sampling points, and the final point is processed symmetrically. Then, the average of the five sampling points within each sliding window is taken to obtain the smoothed velocity data. The smoothed velocity data can be used to calculate the acceleration by comparing the velocity difference between the two sampling points before and after. Finally, by outputting the processed velocity curve and acceleration data, the elimination of measurement noise can be achieved [8]. The entire process ensures the smoothness of the data while avoiding signal distortion. The hidden layer adopts a fully connected approach, with each layer containing 128 neurons, and uses ReLU activation function (AF) to strengthen nonlinear expression ability, as shown in formula (2).

$$\begin{cases} \mathbf{h}_l = \text{ReLU}(\mathbf{W}_l \mathbf{h}_{l-1} + \mathbf{b}_l) \\ \mathbf{W}_1 \in \mathbb{R}^{128 \times 43}, \mathbf{W}_2 \in \mathbb{R}^{128 \times 128}, \mathbf{b}_l \in \mathbb{R}^{128} \\ \text{ReLU}(x) = \max(0, x) \end{cases} \quad (2)$$

In formula (2), \mathbf{h}_l represents the output vector of the l th hidden layer, ReLU represents the modified linear unit AF, \mathbf{W}_l and \mathbf{b}_l represent the weight matrix and the bias vector of the l th layer, respectively [9]. The output layer uses a linear AF to map the hidden layer features to the instantaneous traction power prediction value, as shown in formula (3).

$$\begin{cases} p(t) = \mathbf{W}_o \mathbf{h}_2 + b_o \\ \mathbf{W}_o \in \mathbb{R}^{1 \times 128}, b_o \in \mathbb{R} \end{cases} \quad (3)$$

In formula (3), $p(t)$ represents the instantaneous traction power prediction value at time t , \mathbf{W}_o is the weight matrix of the output layer, \mathbf{h}_2 is the output vector of the second hidden layer, and b_o is the bias term of the output layer [10]. The model's training is executed employing the Adam optimizer, with a learning rate of $\alpha=0.001$ and a batch size of $B=64$. The mean square error is utilized as the loss function, as denoted in formula (4).

$$\mathcal{L}(\theta) = \frac{1}{N} \sum_{k=1}^N (p_k - \hat{p}_k)^2 \quad (4)$$

In formula (4), θ represents all trainable parameters, N denotes the sample size, p_k denotes the predicted power, and \hat{p}_k denotes the measured power. Furthermore, to prevent overfitting, the study also added Dropout technology to the hidden layer, setting the dropout rate to 0.2, as shown in formula (5).

$$\mathbf{h}_l^{\text{train}} = \mathbf{h}_l \odot \mathbf{m}_l, \mathbf{m}_l \sim \text{Bernoulli}(1 - p) \quad (5)$$

In formula (5), \mathbf{m}_l represents the mask vector. Based on the above, the prediction of train EC can be achieved.

2.2 PSO-based Optimization of Train Interval Running Time

Although FNN can be used to predict the EC of urban train traction, pure EC prediction cannot be directly converted into energy-saving operation solutions. The main reason is the Automatic Train Operation (ATO) used by URT, as shown in Fig. 3.

The internal structure of ATO is illustrated schematically in Fig. 3. From the Fig., the ATO system adopts a layered architecture design, which includes two core modules: optimization layer and control layer. In the optimization layer, the recommended speed curve calculation module needs to comprehensively process schedule information, dynamic parameters, and infrastructure data [11]. At the control layer, the speed curve following module is responsible for generating specific control instructions based on vehicle data and real-time operating status. This complex system architecture determines that energy-saving optimization is essentially a complex decision-making problem with multiple objectives and

constraints, requiring comprehensive consideration of optimization requirements from multiple dimensions such as EC characteristics, operational efficiency, and service quality. The PSO algorithm has its core idea derived from simulating the foraging behavior of bird flocks, as shown in Fig. 4.

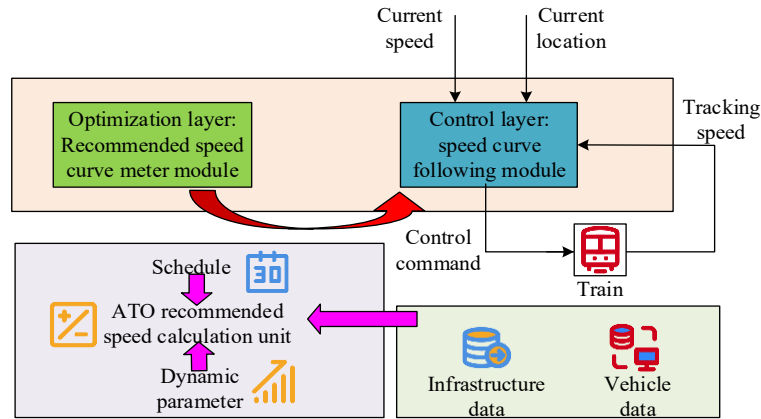


Fig. 3 Schematic diagram of the internal structure of ATO (Fig. source: <https://freeicons.io/iconset/free-icons-set>)

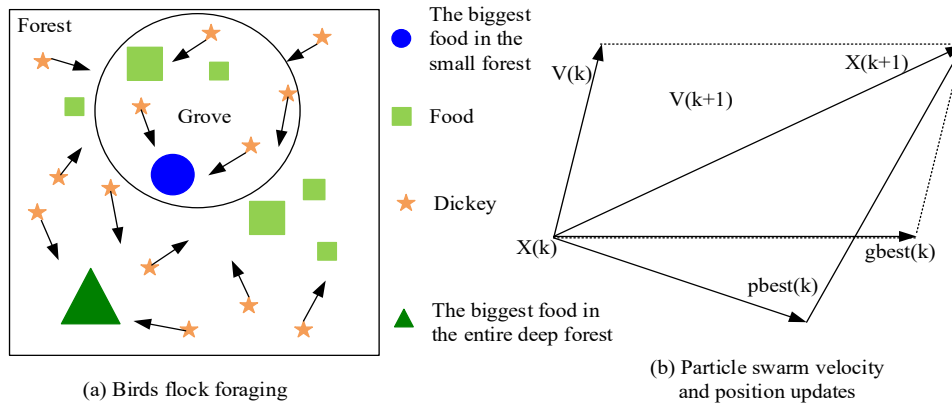


Fig. 4 Schematic diagram of PSO algorithm (Fig. source: self drawn by the author)

Fig. 4 is a schematic diagram of the PSO algorithm, from which it can be seen that PSO simulates bird foraging behavior by maintaining a particle swarm. In the solution space, each particle has two properties: position and velocity. The position vector is representative of a potential optimization solution, with the velocity vector determining the search direction and step size. During the iteration process, particles dynamically adjust their motion trajectories based on their individual historical best position (pbest) and group global best position (gbest), balancing global exploration and local development [12-13]. Based on this, the study proposes to use PSO for multi-objective optimization of the running time of URT train sections. Based on the interval running time EC relationship curve output

by the FNN EC model, the modeling of optimization problems can be achieved, as shown in formula (6).

$$\begin{cases} \delta \mathbf{t} = [\delta t_1, \delta t_2, \dots, \delta t_n]^T \\ f(\delta \mathbf{t}) = k_1 \cdot \frac{E_0 - E(\delta \mathbf{t})}{E_0} + k_2 \cdot \frac{T_0 - T_p(\delta \mathbf{t})}{T_0} + k_3 \cdot \frac{1}{1 + \sum F_i |\sum_{j=1}^i \delta t_j|} \end{cases} \quad (6)$$

In formula (6), $\delta \mathbf{t}$ represents the adjustment amount of running time for each section, $E(\delta \mathbf{t})$ represents the predicted traction EC of the entire line through the FNN model, $T_p(\delta \mathbf{t})$ represents the average passenger travel time, δt_i is the weight coefficient, F_i represents the identification of transfer stations, and 1 is a transfer station and 0 is a non transfer station. After modeling the optimization problem of train interval running time, PSO algorithm can be used to solve it. Considering that the standard PSO lacks an effective constraint handling mechanism, it is difficult to ensure an operational constraint where the sum of time adjustments in each interval is zero. In addition, the search strategy with fixed parameters for standard PSO cannot adapt to the changing requirements at different stages of the optimization process, which may lead to the inability to obtain effective solutions in the end [14]. Based on this, research has improved PSO. Firstly, a discretization mechanism is designed and a rounding function is introduced to map the continuous solution space to an integer adjustment of [-10,10] seconds, as shown in formula (7).

$$\delta t_i = \text{round}(x_i), x_i \in [-10,10], \delta t_i \in \mathbb{Z} \quad (7)$$

In formula (7), x_i represents the position component of the continuous space, and δt_i is the discretized time adjustment. Secondly, a dual constraint handling mechanism is developed. The reflection method is used to handle the amount of transgressive adjustments in individual intervals, while the iterative repair operator ensures that the adjustments in each interval sum to zero, as shown in formula (8).

$$\begin{cases} x_i^{new} = \begin{cases} 2 \cdot x_{min} - x_i & \text{if } x_i < x_{min} \\ 2 \cdot x_{max} - x_i & \text{if } x_i > x_{max} \\ x_i & \text{otherwise} \end{cases} \\ \Delta = \sum_{i=1}^n \delta t_i, \delta t_i^{adj} = \delta t_i - \text{sign}(\Delta) \cdot \frac{|\Delta|}{n} \end{cases} \quad (8)$$

In formula (8), x_i^{new} represents the new position value after reflection processing, and x_{min} and x_{max} respectively represent the allowed minimum and maximum adjustment amounts [15]. Δ represents the deviation between the current total adjustment amount and zero, n means the total amount of intervals, and δt_i^{adj} means the corrected adjustment amount. Finally, an adaptive parameter system is constructed to achieve a dynamic balance between search breadth and accuracy, as shown in formula (9).

$$\begin{cases} w(t) = w_{max} - \frac{t}{T_{max}}(w_{max} - w_{min}) \\ v_{id}^{k+1} = w(t)v_{id}^k + 1.5r_1(pbest_{id} - x_{id}^k) + 1.5r_2(gbest_d - x_{id}^k) \end{cases} \quad (9)$$

In formula (9), $w(t)$ means the inertia weight at the t -th iteration, T_{max} means the maximum number of iterations, v_{id}^k is the velocity of the i -th particle in the d -th dimension at the k th generation, r_1 and r_2 represent random numbers uniformly distributed in the $[0,1]$ interval, $pbest_{id}$ is the historical optimal position of the i th particle, and $gbest_d$ is the global optimal position of the population.

2.3 Optimization of Urban Rail Train Strategy Based on PPO

Although the enhanced PSO algorithm can optimize the running time of urban rail train sections, this static optimization method grounded on a fixed timetable is difficult to adapt to the dynamic changes in actual operation. Specifically, URT systems typically face three types of dynamic uncertainties during operation. One is the real-time fluctuation of train operation status, such as changes in traction system efficiency. The second is external environmental disturbances, such as sudden changes in passenger flow. Finally, there is the dynamic evolution of infrastructure status, such as temporary speed limits on tracks. PPO, as a policy gradient algorithm, has a unique ability to handle continuous decision problems and adapt to dynamic environments. The specific structure of PPO is denoted in Fig. 5.

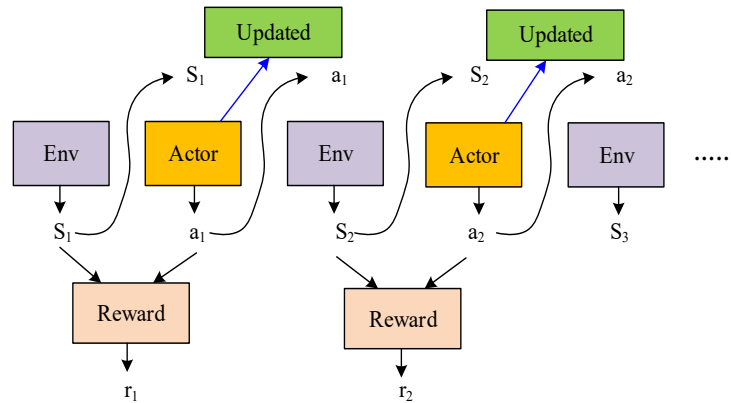


Fig. 5 PPO algorithm structure (Fig. source: self drawn by the author)

Fig. 5 showcases the structure of the PPO algorithm. From the Fig., the core architecture of the PPO algorithm consists of four parts: the policy network (Actor), the value network (Critic), the replay buffer, and the clipped surrogate objective mechanism [16-17]. Based on this structure, the sampled data can undergo multiple policy updates while also being able to control the magnitude of the updates. Based on this research, it is proposed to introduce PPO algorithm on the basis of PSO static optimization and construct a two-layer control architecture of "static optimization+dynamic adjustment", as shown in Fig. 6.

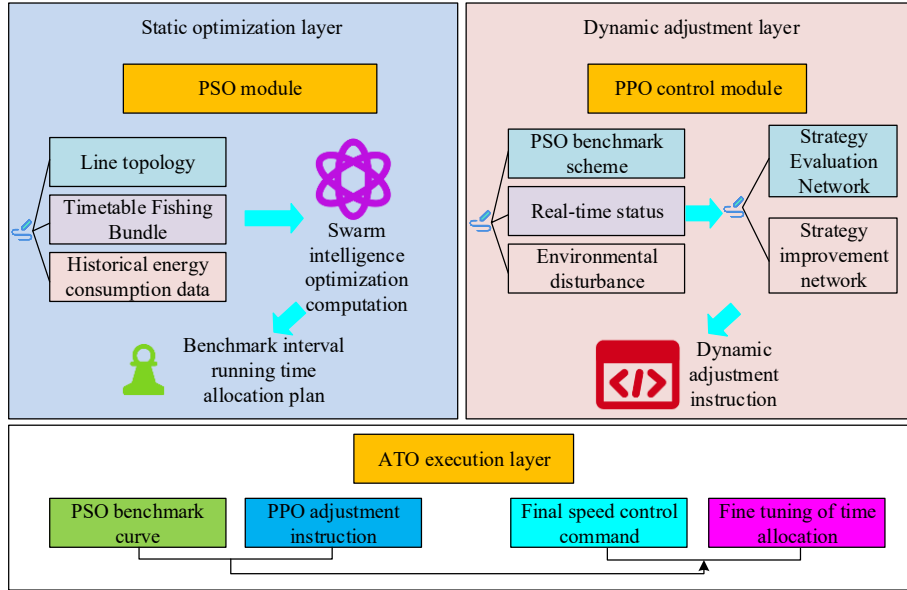


Fig. 6 Dual layer control architecture (Fig. source: <https://freeicons.io/iconset/free-icons-set>)

Fig. 6 is a schematic diagram of the dual layer control architecture of PSO-PPO. From the figure, the framework adopts a dual branch network structure design, where the main branch is responsible for generating the basic parameters of the recommendation speed curve, and the auxiliary branch outputs the dynamic adjustment of the running time. This structure not only retains the benchmark value of PSO optimization results, but also endows the system with the ability to adjust in real-time [18]. During the strategy update process, PPO ensures training stability by minimizing the following pruning objective function, as shown in formula (10).

$$\mathcal{L}^{CLIP}(\theta) = \mathbb{E}_t[\min(r_t(\theta)\hat{A}_t, \text{clip}(r_t(\theta), 1 - \epsilon, 1 + \epsilon)\hat{A}_t)] \quad (10)$$

In formula (10), $r_t(\theta)$ represents the ratio of new and old strategies, \hat{A}_t is the estimated value of the advantage function, and ϵ represents the clipping parameter. In addition, in the state space design, static features and real-time dynamic parameters from PSO optimization results are integrated, including current speed deviation, remaining interval distance, instantaneous EC rate, etc. The action space adopts a hybrid design, with continuous actions corresponding to the adjustment parameters of the velocity curve, and discrete actions representing the fine-tuning amount of time allocation. This design not only meets the control requirements of the ATO system, but also maintains the flexibility of the strategy, ultimately enabling the system to autonomously adjust the control strategy based on real-time operating status.

3. Results

3.1. Performance Verification of Optimization Model for Urban Rail Trains

To comprehensively evaluate the performance of the proposed FNN-PSO-PPO integrated optimization model, the study validated it. The experimental data was based on the actual operation data of a new first tier city's subway line 4, collected from January 2022 to January 2023. A typical line segment containing 10 stations and 9 sections was selected as the test object. To better demonstrate the effect of the research model, a comparative method was used in the experiment, which included the traditional Physics-based Heuristic method (PH) that calculates EC based on physical models and combines heuristic time adjustment, and the Long Short-Term Memory-Genetic Algorithm (LSTM-GA) as the comparative model. The parameter settings of each model are denoted in Table 1.

Table 1

Parameter settings			
Parameter group	FNN-PSO-PPO	LSTM-GA	PH method
Energy consumption model	3-layer FNN	2-layer LSTM	Physical equations
Optimization algorithm	PSO+PPO	Genetic algorithm (GA)	Heuristic rules
Dynamic adjustment	Real-time policy	None	None

Table 1 shows the parameter settings for each model. Based on the above parameter settings, the study conducted tests under two different operating conditions. The first scenario was a normal working condition, and the second scenario was a dynamic disturbance scenario (mainly in the case of sudden passenger flow). The experiment first tested the performance of each model under normal operating conditions, as shown in Fig. 7.

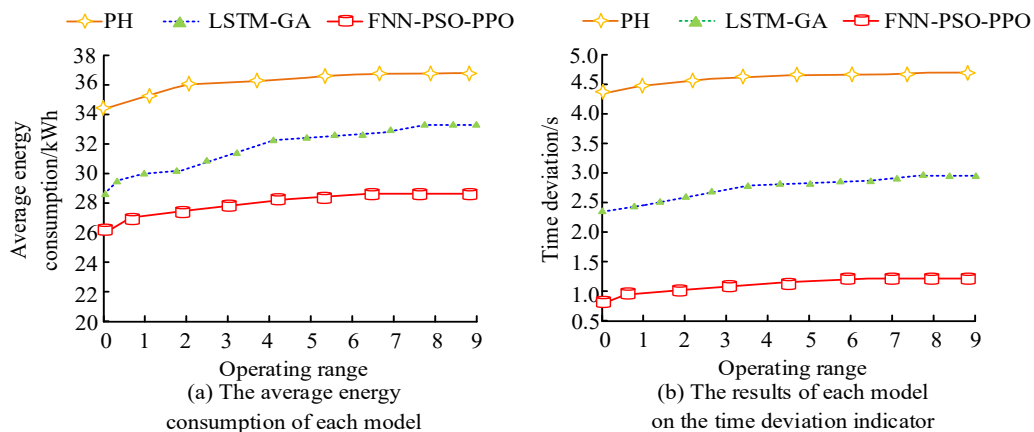


Fig. 7. Performance under normal operating conditions (Fig. source: self drawn by the author)

Fig. 7 shows the performance under normal operating conditions. Among them, Fig. 7 (a) showcases the average EC of each model. From the Fig., the average EC of the PH model was 35.7kWh, and the average EC of the LSTM-GA model was 32.1kWh. In contrast, the FNN-PSO-PPO model designed by the research had the lowest average EC, at 28.5 kWh. Fig. 7 (b) shows the results of each model on the time deviation index. From the Fig., the PH model had the largest time deviation value of 4.5s. The LSTM-GA model was the second with a time deviation value of 2.8s. In contrast, the FNN-PSO-PPO model had the smallest time deviation value of 1.2s. Under dynamic disturbance scenarios, the performance of each model can be seen in Fig. 8.

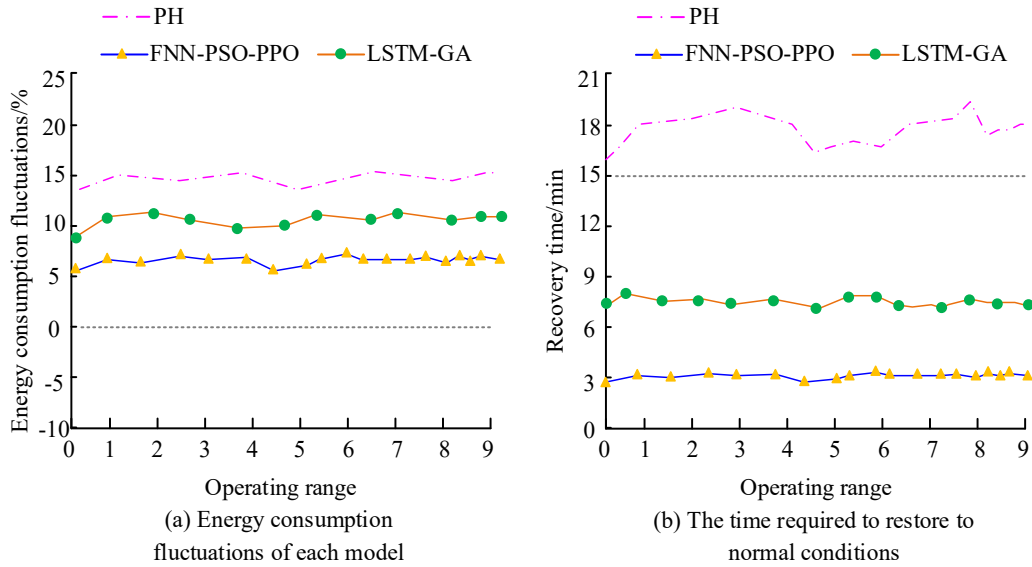


Fig. 8. Performance under dynamic disturbance scenario (Fig. source: self drawn by the author)

Fig. 8. shows the performance under dynamic disturbance scenarios. Among them, Fig. 8 (a) showcases the EC fluctuations of each model. From the Fig., in the scenario of sudden increase in passenger flow, the EC fluctuation value of the PH model was +15.3%, and the EC fluctuation value of the LSTM-GA model was +11.5%. In contrast, the FNN-PSO-PPO model had the smallest EC fluctuation range, which was +6.2%. Fig. 8 (b) shows the time required for each model to recover to normal under the scenario of sudden increase in passenger flow. From the Fig., the recovery time of the PH model needed to be at least 15 minutes, while the recovery time of the LSTM-GA model was 8.2 minutes. In contrast, the FNN-PSO-PPO model required the shortest recovery time, only 3.1 minutes. Overall, in the above two operating conditions, the FNN-PSO-PPO model designed by the research has the best overall performance.

3.2 Example Testing of Optimization Model for Urban Rail Trains

To test the applicability of the FNN-PSO-PPO model in practical operation scenarios, field tests were conducted on Beijing Metro Line 14 (Shangezhuang Zhangguozhuang section), which was 28.3 kilometers long, had 21 stations, and included typical urban rail features such as steep slopes and small radius curves. The test was conducted during the morning and evening peak hours (7:00-9:00, 17:00-19:00) on weekdays from May to June 2023, with a focus on examining the performance of the model under high passenger flow density. The experiment used the current PID control strategy of the circuit as a benchmark for comparison. Traction EC data was collected through a vehicle mounted energy metering device (with an accuracy of $\pm 0.5\%$), and the signal system recorded the running time parameters at a resolution of 0.1 seconds. At the same time, temperature and humidity sensors were configured to monitor the environmental status, and a complete multi-dimensional data acquisition system was constructed. During the testing process, the model control instructions interacted in real-time with the actual operating data to ensure that the testing conditions are highly consistent with the actual operating conditions. The experiment first tested the basic performance during the off peak period, and the results are shown in Fig. 9.

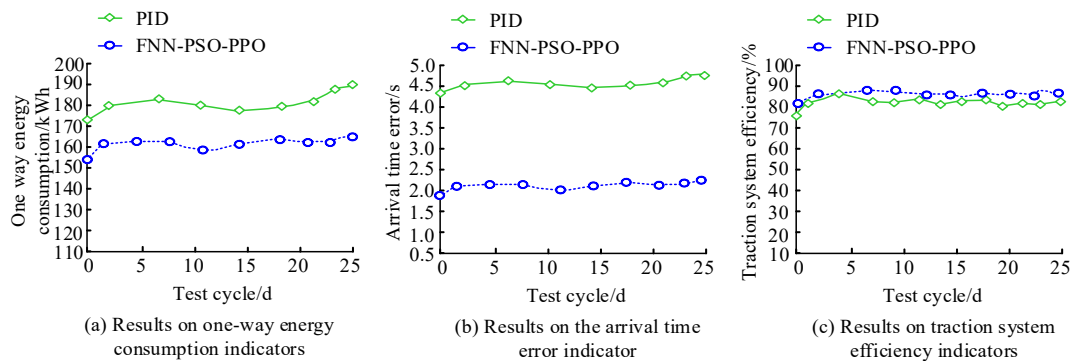


Fig. 9. Basic performance during the off peak period (Fig. source: self drawn by the author)

Fig. 9 shows the basic performance during the off peak period. Fig. 9 (a) shows the results on the one-way EC index. From the Fig., under the current PID control strategy, the one-way EC of the train was 188.5 kWh, while after using the FNN-PSO-PPO model, its one-way EC was reduced to 162.3 kWh. Fig. 9 (b) showcases the results on the arrival time error index. From the Fig., under the current PID control strategy, the arrival time error of the train was 4.7s, while after using the FNN-PSO-PPO model, its arrival time error was reduced to 2.1s. Fig. 9 (c) shows the results on the traction system efficiency index. From the Fig., under the current PID control strategy, the traction system efficiency was 83.7%, while in

the FNN-PSO-PPO model, the traction system efficiency was 89.2%. In addition, the study also examined the compressive performance of the model during the morning rush hour, as shown in Fig. 10.

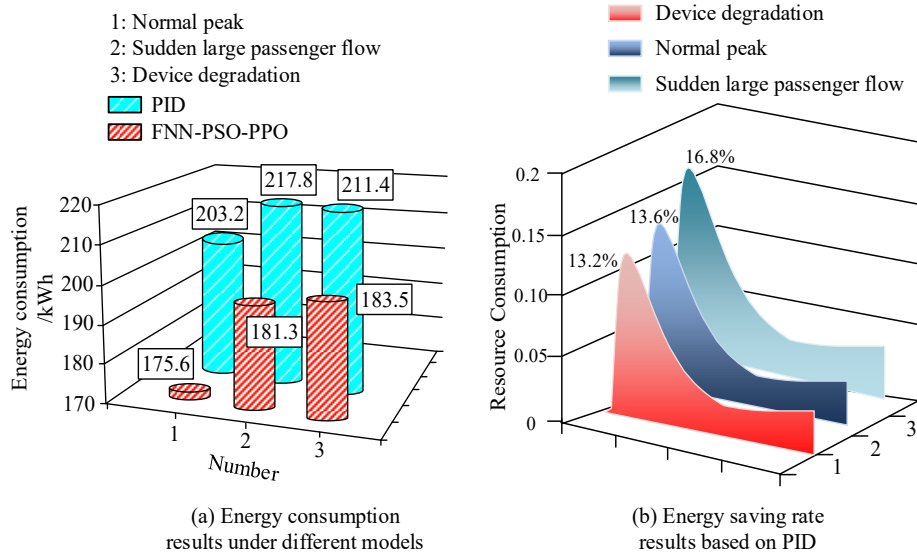


Fig. 10. Results of morning peak stress test (Fig. source: self drawn by the author)

Fig. 10 shows the results of the morning peak stress test. Fig. 10 (a) shows the EC results under different models. From the Fig., in the normal peak scenario, the EC under PID control was 203.2 kWh, and the EC of the FNN-PSO-PPO model was 175.6 kWh. In the scenario of sudden large passenger flow, the EC under PID control was 217.8 kWh, and the EC of the FNN-PSO-PPO model was 181.3 kWh. In the scenario of device degradation, the EC under PID control was 211.4 kWh, and the EC of the FNN-PSO-PPO model was 183.5 kWh. Fig. 10 (b) shows the energy-saving rate results obtained based on PID. From the Fig., under normal peak conditions, the energy-saving rate reached 13.6% after using the FNN-PSO-PPO model. In the case of sudden large passenger flow, the use of the FNN-PSO-PPO model resulted in an energy saving rate of 16.8%. In the scenario of device degradation, after using the FNN-PSO-PPO model, the energy saving rate reached 13.2%. Furthermore, the study conducted a comprehensive benefit evaluation of the model, and the outcomes are denoted in Table 2. Table 2 shows the comprehensive benefit evaluation results. From the table, in terms of energy economy, the average annual power consumption of a single train was reduced to 58.6 megawatt hours, which was 14.3% lower than traditional PID control, equivalent to saving 32000 yuan in electricity bills per train per year.

Table 2

Comprehensive benefit evaluation

Evaluation dimension	Specific metrics	FNN-PSO-PPO	Conventional PID	Improvement	Economic value conversion
Energy economics	Annual energy consumption per train (MWh)	58.6	68.4	-14.30%	\$4,900 savings
	Peak power demand (kW)	1,850	2,150	-14.00%	Reduced capacitor upgrade cost
Operational efficiency	Daily punctuality rate (%)	99.2	97.8	+1.4pp	Reduced delay penalties \$27,600
	Average turnaround time (min)	92.4	95.1	-2.80%	226 additional annual trips
Equipment maintenance	Brake pad replacement cycle (months)	9.5	7.2	31.90%	\$6,900 material savings
	Traction motor failure rate (incidents/year)	1.2	2.7	-55.60%	\$10,400 maintenance savings
Environmental benefits	Annual CO ₂ reduction (tons)	46.2	-	-	Carbon trading value \$1,700
	Noise reduction (dB)	3.2	-	-	Improved environmental rating

The peak power demand decreased by 14% from 2150 kW to 1850 kW, effectively reducing the cost of capacitor expansion. According to the operational efficiency dimension, the daily punctuality rate increased by 1.4% to 99.2%, and the average turnover time was shortened by 2.8% to 92.4 minutes. Based on this, it is estimated that the entire line can increase 226 trips per year. In terms of equipment maintenance, the replacement cycle of brake pads has been extended from 7.2 months to 9.5 months, and the failure rate of traction motors has been reduced by 55.6% to 1.2 times per year. In terms of environmental benefits, annual CO₂ emission reduction of 46.2 tons and noise pollution reduction of 3.2 decibels were realized. According to calculations, the annual comprehensive benefit of a single train was 336000 yuan. Based on the operation scale of 42 trains on Beijing Metro

Line 14, the annualized benefit of the entire line could reach 14.11 million yuan, with an investment recovery period of about 2.3 years. Overall, the model proposed by the research has good practical application value.

4. Discussion and conclusion

In order to improve the energy efficiency and running time accuracy of urban rail trains and enhance the adaptability of the system under dynamic disturbance, an integrated optimization model based on FNN-PSO-PPO is proposed. The experimental results show that under normal conditions, the average energy consumption of the model is reduced to 28.5kwh, which is 20.2% lower than the traditional physical model and 11.2% lower than the LSTM-GA model. This result is significantly better than the performance of the traditional static optimization method, reflecting the comprehensive advantages of FNN-PSO-PPO model in energy consumption prediction and optimization. In terms of time accuracy, the time deviation of the research model is only 1.2 seconds, which is 3.3 seconds less than 4.5 seconds of the traditional method. This result not only meets the strict requirements of urban rail transit for high punctuality rate, but also significantly improves the travel experience of passengers. In addition, in the dynamic disturbance scenario, fnn-pso-ppo model can stably control the fluctuation range of energy consumption at 6.2%, which is better than 11.5% of lstm-ga model, and shorten the recovery time to 3.1 minutes. This rapid response ability is particularly important in scenarios such as sudden passenger flow or equipment failure, and can effectively avoid the operation interruption caused by disturbance. The actual operation test further verifies the comprehensive performance of the model. The FNN-PSO-PPO model can reduce the one-way energy consumption by 13.6% to 16.8%, improve the punctuality rate to 99.2%, and improve the efficiency of the traction system to 89.2% in the tests of the peak period and peak period. These improvements not only improved the operation efficiency, but also brought significant economic benefits. The annual comprehensive economic benefits of a single train reached 336000 yuan, and the annual benefits of the whole line reached 14.11 million yuan. In addition, the performance of the model in terms of equipment maintenance and environmental benefits is also outstanding. For example, the replacement cycle of brake pads is extended to 9.5 months, the failure rate of traction motor is reduced by 55.6%, and the annual CO₂ emission reduction is 46.2 tons. These results fully reflect the comprehensive advantages of the research model in energy saving, punctuality, dynamic adaptability and economy.

Compared with the same type of research, Hussain et al. [19] analyzed 11 machine learning models (including ridge regression, Lasso regression, k nearest neighbor, gradient lifting, support vector regression, multi-layer perceptron XGBoost, CatBoost, LightGBM, the performance of Gauss process regression

(GPR) and additional tree regression (ATR) in energy consumption prediction was systematically evaluated. The results showed that the ATR performed best in prediction accuracy (MAE=0.5888, $R^2=0.9592$). However, these models still have limitations in capturing the nonlinear characteristics under extreme conditions, especially for complex dynamic systems. In contrast, the proposed fnn-pso-ppo framework achieves better performance by integrating the feature extraction ability of deep neural network and the dynamic optimization characteristics of reinforcement learning. Although the LSTM model developed by Wu et al. [20] achieves a prediction error of less than 2% and a fast response of 0.95 seconds, its application scenario is limited to the static energy consumption prediction of new energy vehicles. The advantage of this study is to build a complete "prediction static optimization dynamic adjustment" closed-loop system, which not only considers the accuracy of energy consumption prediction, but also solves the unique dynamic optimization problem of rail transit, so as to achieve higher comprehensive performance in complex operation environment. Overall, the proposed model has unique value in solving the multi-objective optimization problem of urban rail transit.

However, there is still room for improvement. The research assumes that the dynamic disturbance during train operation can be monitored in real time and accurately input into the model, but in actual operation, the accuracy of sensors and data transmission delay may affect the dynamic adjustment effect of the model. Therefore, in the future, we can consider introducing multi-source information fusion algorithm to integrate multimodal data from video surveillance, Wi Fi probe, on-board diagnosis system and so on, so as to improve the accuracy of disturbance identification.

Fundings

The research is supported by: Xi'an Science and Technology Bureau Science and Technology Personnel Service Enterprise Project: Research on Energy saving System of Urban Rail Transit Train Based on Optimization Algorithm (No.:24GXFW0044).

R E F E R E N C E S

- [1] Hasanzadeh S, Zarei S F, Najafi E. A train scheduling for energy optimization: Tehran metro system as a case study. *IEEE Transactions on Intelligent Transportation Systems*, 2022, 24(1): 357-366.
- [2] Cao Y, Zhang Z, Cheng F, Su S. Trajectory optimization for high-speed trains via a mixed integer linear programming approach. *IEEE Transactions on Intelligent Transportation Systems*, 2022, 23(10): 17666-17676.

- [3] Novak H, Lešić V, Vašak M. Energy-efficient model predictive train traction control with incorporated traction system efficiency. *Ieee transactions on intelligent transportation systems*, 2021, 23(6): 5044-5055.
- [4] Su S, Zhu Q, Liu J, Tang T, Wei Q, Cao Y. A data-driven iterative learning approach for optimizing the train control strategy. *IEEE Transactions on Industrial Informatics*, 2022, 19(7): 7885-7893.
- [5] Haldorai A, Ramu A. Canonical correlation analysis based hyper basis feedforward neural network classification for urban sustainability. *Neural Processing Letters*, 2021, 53(4): 2385-2401.
- [6] Jie Li, Runkai Hua. Based on multi-agent systems for subway train energy-efficient operation optimization. *Advances In Industrial Engineering and Management*, 2024, 13(3)
- [7] Khan J, Lee E, Kim K. A higher prediction accuracy-based alpha-beta filter algorithm using the feedforward artificial neural network. *CAAI Transactions on Intelligence Technology*, 2023, 8(4): 1124-1139.
- [8] Pratap Mukherjee R, Kumar Roy P, Kumar Pradhan D. An Efficient FNN model with chaotic oppositional based SCA to solve classification problem. *IETE Journal of Research*, 2023, 69(7): 4205-4223.
- [9] Zhang D G, Yang P, Chen J, Zhang X D, Zhang T. Novel FNN-based machine deep learning approach for image aggregation in application of the IoT. *Journal of Experimental & Theoretical Artificial Intelligence*, 2022, 34(6): 1029-1046.
- [10] Demir S, Sahin E K. Predicting occurrence of liquefaction-induced lateral spreading using gradient boosting algorithms integrated with particle swarm optimization: PSO-XGBoost, PSO-LightGBM, and PSO-CatBoost. *Acta Geotechnica*, 2023, 18(6): 3403-3419.
- [11] Rahayu E S, Ma'arif A, Cakan A. Particle swarm optimization (PSO) tuning of PID control on DC motor. *International Journal of Robotics and Control Systems*, 2022, 2(2): 435-447.
- [12] Minh H L, Khatir S, Rao R V, Wahab M A, Cuong-Le T. A variable velocity strategy particle swarm optimization algorithm (VVS-PSO) for damage assessment in structures. *Engineering with Computers*, 2023, 39(2): 1055-1084.
- [13] El-Shafiey M G, Hagag A, El-Dahshan E S A, Ismail M A. A hybrid GA and PSO optimized approach for heart-disease prediction based on random forest. *Multimedia Tools and Applications*, 2022, 81(13): 18155-18179.
- [14] Pradhan A, Bisoy S K, Das A. A survey on PSO based meta-heuristic scheduling mechanism in cloud computing environment. *Journal of King Saud University-Computer and Information Sciences*, 2022, 34(8): 4888-4901.
- [15] Hebba C, Mamatha H. Comprehensive Dataset Building and Recognition of Isolated Handwritten Kannada Characters Using Machine Learning Models. *Artificial Intelligence and Applications*, 2023, 1(3):179-190.
- [16] Cheng Y, Huang L, Wang X. Authentic boundary proximal policy optimization. *IEEE Transactions on Cybernetics*, 2021, 52(9): 9428-9438.
- [17] Mayer S, Classen T, Endisch C. Modular production control using deep reinforcement learning: proximal policy optimization. *Journal of Intelligent Manufacturing*, 2021, 32(8): 2335-2351.
- [18] Ying C S, Chow A H F, Wang Y H, Chin K S. Adaptive metro service schedule and train composition with a proximal policy optimization approach based on deep reinforcement learning. *IEEE Transactions on Intelligent Transportation Systems*, 2021, 23(7): 6895-6906.

- [19] Hussain I, Ching B K, Utraphan C, Tay K G, Noor A. Evaluating machine learning algorithms for energy consumption prediction in electric vehicles: A comparative study. *Scientific reports*, 2025, 15(1):16124.
- [20] Wu S, Wang F, Wan M. Energy consumption prediction of new energy vehicles in smart city based on LSTM network. *International Journal of Global Energy Issues*, 2022, 44(5-6):484-497.